

Contribution from the Corporate Research Science Laboratory, Exxon Research and Engineering Company, Annandale, New Jersey 08801, Department of Materials Science, Stanford University, Stanford, California 94305, Department of Biochemistry, University of Georgia, Athens, Georgia 30602, and School of Chemical Sciences, University of Illinois, Urbana, Illinois 61801

X-ray Absorption Spectroscopic Evidence for a Unique Nickel Site in *Clostridium thermoaceticum* Carbon Monoxide Dehydrogenase

Stephen P. Cramer,^{*1a,b} Marly K. Eidsness,^{1c,d} W.-H. Pan,^{1a} Thomas A. Morton,^{1e} Steve W. Ragsdale,^{1e,f} Daniel V. DerVartanian,^{1e} Lars G. Ljungdahl,^{1e} and Robert A. Scott^{*1g}

Received November 4, 1986

Carbon monoxide dehydrogenase (COdH) in *Clostridium thermoaceticum* is an $\alpha_3\beta_3$ protein containing six nickels per molecule, in addition to a number of Fe-S clusters. Previous electron paramagnetic resonance (EPR) spectroscopic work has suggested that nickel is involved in binding CO forming an EPR-detectable species, which is probably a key intermediate in the oxidation of CO to CO₂ and in the synthesis of acetate. In order to better define the nature of this nickel site, Ni X-ray absorption spectra have been recorded and interpreted by comparison with model compounds. The extended X-ray absorption fine structure (EXAFS) spectrum for oxidized COdH is different from that of other Ni enzymes. Both the EXAFS and the X-ray absorption edge spectra suggest a Ni site containing substantial sulfur ligation. The Ni X-ray absorption edge spectrum of rubredoxin-oxidized COdH exhibits a characteristic shoulder with an inflection point at 8336 eV. Such a feature is absent in octahedral model compounds, whereas a well-resolved peak is observed in square-planar Ni complexes. A distinct 1s \rightarrow 3d transition at 8333 eV is observed in a tetrahedral model. The lack of correspondence suggests that square-pyramidal and distorted-square-planar geometries are plausible candidates for the COdH Ni site. Treatment of rubredoxin-oxidized COdH with hydrogenase and H₂ shifts the Ni edge to lower energies, indicating Ni-based reduction.

Introduction

Carbon monoxide dehydrogenase (COdH²), first found in *Clostridium thermoaceticum* by Diekert and Thauer,³ catalyzes the oxidation of CO to CO₂ with a variety of electron acceptors.⁴ More importantly, it catalyzes an exchange reaction between CO and the carbonyl group of acetyl-CoA.⁵ This exchange reaction requires that COdH bind the three moieties methyl, carbonyl, and CoA. COdH is therefore the enzyme that catalyzes the final step of acetyl-CoA synthesis from one-carbon precursors in acetogenic bacteria.⁵⁻⁷ COdH contains nonequivalent α and β subunits with respective molecular masses of 78 000 and 71 000 Da.⁴ Each $\alpha\beta$ dimer contains approximately 2 nickel atoms, 1 zinc atom, 11 iron atoms, and 14 acid-labile sulfur atoms.⁴ Although the Ni site is EPR-silent in the oxidized and reduced states of the enzyme, a rhombic EPR signal is induced by addition of CO or HCO₃⁻/CO₂ to the oxidized enzyme.⁸ Isotopic substitution of ⁶¹Ni or ⁵⁷Fe causes a significant change in this substrate-induced EPR signal,⁸ indicating that the active site of COdH is a spin-coupled center involving both Ni and Fe atoms. In order to better define the nature of the nickel site in this enzyme, preliminary X-ray absorption spectroscopic results are reported herein.

Experimental Section

Enzyme Purification and Sample Preparation. CO dehydrogenase from *C. thermoaceticum* was purified under anaerobic conditions by

published procedures,⁴ with the exception that gel filtration was replaced by Phenyl Sepharose chromatography using a decreasing gradient of ammonium sulfate concentration, 0.4-0 M, and an increasing glycerol gradient, 0-20%. The enzyme eluted at approximately 150 mM (N-H₄)₂SO₄, 12% glycerol, and was then applied to the Biogel HTP column as described previously.⁴ The enzyme as isolated was in a buffer of 50 mM Tris/HCl, pH 7.6, or KP_i, pH 6.8, containing 2 mM sodium dithionite. It was concentrated to approximately 40 mg/mL by using an Amicon XM-100 ultrafiltration membrane. Buffer changes or removal of reducing substances were done on a 20-mL Sephadex G-25 column equilibrated with the appropriate buffer. The samples were then further concentrated and either loaded directly into Lucite XAS cells or incubated under H₂ or CO for 45 min before loading. The samples were then immediately frozen and stored in liquid nitrogen.

The COdH samples used herein had a specific activity of 340 units/mg. The enzyme was concentrated to 300 mg of protein/mL and had a nickel concentration of 3.31 mM. All samples were in 50 mM Tris/HCl, pH 7.6, with no dithionite. One sample of the enzyme was reduced by the addition of hydrogenase (0.8 mg containing 860 units) and incubation under H₂. The hydrogenase was purified from *Acetobacterium woodii* and has been shown to reduce the iron-sulfur clusters of COdH in the presence of H₂. Unlike some other hydrogenases, it does not contain nickel.⁹ Two enzyme samples were oxidized by the addition of oxidized rubredoxin¹⁰ (1.77 mol of rubredoxin/mol of hexamer), which has been shown to be an excellent electron acceptor from COdH.⁴ One of the oxidized enzyme samples was reacted with CO, which produced an EPR-active species at a concentration of 1.6 mM, representing 48% of the nickel.

Nickel Model Compounds. The nickel model compounds used in this study were [Ni^{II}(Et₂dtc)₂] (Et₂dtc \equiv diethyldithiocarbamate),¹¹ Ni^{II}(ibc) (ibc \equiv 1,2-dihydromethylmesopyropheophorbide *a*, an isobacteriochlorin-like macrocycle),¹² [(*n*-C₄H₉)₄N]₂[Ni^{II}(mnt)₂] (mnt \equiv maleonitriledithiolate),¹³ [Ni^{II}(en)₃]Cl₂ (en \equiv ethylenediamine),¹⁴ [Ni^{II}([9]-aneS₃)₂](ClO₄)₂ ([9]aneS₃ \equiv 1,4,7-trithiacyclononane),¹⁵ and [(C₆H₅)₄P]₂[Ni^{II}(SC₆H₅)₄].¹⁶ The preparation procedure and the XAS data for the other nickel enzymes, *S*-methyl coenzyme-M reductase from *Meth-*

- (1) (a) Exxon Research and Engineering Co. (b) Present address: Schlumberger-Doll Research, Ridgefield, CT 06877-4108. (c) Stanford University. (d) Present address: School of Chemical Sciences, University of Illinois, Urbana, IL 61801. (e) University of Georgia. (f) Present address: Department of Chemistry, University of Wisconsin-Milwaukee, Milwaukee, WI 53201. (g) University of Illinois.
- (2) Abbreviations: CoA, coenzyme A; COdH, carbon monoxide dehydrogenase; EPR, electron paramagnetic resonance; XAS, X-ray absorption spectroscopy; EXAFS, extended X-ray absorption fine structure; XANES, X-ray absorption near-edge structure.
- (3) Diekert, G.; Thauer, R. K. *J. Bacteriol.* **1978**, *136*, 597-606.
- (4) Ragsdale, S. W.; Clark, J. E.; Ljungdahl, L. G.; Lundie, L. L.; Drake, H. L. *J. Biol. Chem.* **1983**, *258*, 2364-2369.
- (5) Ragsdale, S. W.; Wood, H. G. *J. Biol. Chem.* **1985**, *260*, 3970-3977.
- (6) Ljungdahl, L. G. *Annu. Rev. Microbiol.* **1986**, *40*, 415-450.
- (7) Wood, H. G.; Ragsdale, S. W.; Pezacka, E. *Biochem. Int.* **1986**, *12*, 421-440.
- (8) (a) Ragsdale, S. W.; Ljungdahl, L. G.; DerVartanian, D. V. *Biochem. Biophys. Res. Commun.* **1982**, *108*, 658-663. (b) Ragsdale, S. W.; Ljungdahl, L. G.; DerVartanian, D. V. *Biochem. Biophys. Res. Commun.* **1983**, *115*, 658-665. (c) Ragsdale, S. W.; Wood, H. G.; Antholine, W. E. *Proc. Natl. Acad. Sci. U.S.A.* **1986**, *82*, 6811-6814.

- (9) Ragsdale, S. W.; Ljungdahl, L. G. *Arch. Microbiol.* **1984**, *139*, 361-365.
- (10) Ragsdale, S. W.; Ljungdahl, L. G. *J. Bacteriol.* **1984**, *157*, 1-6.
- (11) Coucouvanis, D. *Prog. Inorg. Chem.* **1970**, *11*, 234-371.
- (12) A gift from Jack Fajer of Brookhaven National Laboratory; Smith, K. M.; Goff, D. A. *J. Am. Chem. Soc.* **1985**, *107*, 4954-4964.
- (13) Davison, A.; Holm, R. H. *Inorg. Synth.* **1967**, *10*, 8-26.
- (14) Curtis, N. F. *J. Am. Chem. Soc.* **1961**, *83*, 3147-3148.
- (15) A gift from K. Wieghardt, Ruhr University, Federal Republic of Germany; Setzer, W. N.; Ogle, C. A.; Wilson, G. S.; Glass, R. S. *Inorg. Chem.* **1983**, *22*, 266-271.
- (16) A gift from D. Coucouvanis, University of Michigan; Swenson, D.; Baenziger, N. C.; Coucouvanis, D. *J. Am. Chem. Soc.* **1978**, *100*, 1932-1934.

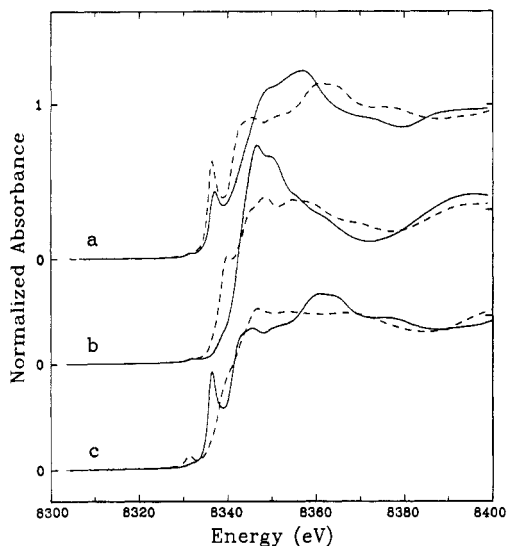


Figure 1. Nickel absorption edge region for some representative Ni-N and Ni-S ligated complexes: (a) $\text{Ni}^{\text{II}}(\text{ibc})$ [square-planar NiN_4] (—) vs. $[\text{Ni}^{\text{II}}(\text{mnt})_2]^{2-}$ [square-planar NiS_4] (---); (b) $[\text{Ni}^{\text{II}}(\text{en})_3]^{2+}$ [octahedral NiN_6] (—) vs. $[\text{Ni}^{\text{II}}(\text{[9]aneS}_3)_2]^{2+}$ [octahedral NiS_6] (---); (c) $[\text{Ni}^{\text{II}}(\text{mnt})_2]^{2-}$ [square-planar NiS_4] (—) vs. $[\text{Ni}^{\text{II}}(\text{SC}_6\text{H}_5)_4]^{2-}$ [tetrahedral NiS_4] (---).

anobacterium thermoautotrophicum, strain ΔH ,¹⁷ and the hydrogenase from *Desulfovibrio gigas*¹⁸ have been previously described.

Data Collection and Processing. The X-ray absorption spectra were recorded at the Stanford Synchrotron Radiation Laboratory (SSRL) by using transmission mode for the model compound spectra and filtered fluorescence detection¹⁹ with elemental cobalt filters for the enzyme spectra. Three ionization chambers with N_2 gas were used, with the first ionization chamber defining I_0 and a metal foil between the second and third chambers acting as an internal energy calibrant. The spectra were calibrated by using 8331.6 eV for the nickel foil first inflection point. The X-ray absorption edge spectra were normalized by setting the extrapolated value of a spline fit to the EXAFS to unity at 8350 eV.

The EXAFS spectra were extracted and processed according to previously described procedures.^{20–24} Empirical phase shifts were obtained from the model compounds $[\text{Ni}^{\text{II}}(\text{en})_3]\text{Cl}_2$ and $[(n\text{-C}_4\text{H}_9)_4\text{N}]_2[\text{Ni}^{\text{II}}(\text{mnt})_2]$ for Ni-N and Ni-S interactions, respectively. Theoretical amplitude functions²⁵ were used to estimate the model compound Debye-Waller factors, which then permitted definition of the empirical amplitude functions. A constant E_0 of 8350 eV was used for all Ni EXAFS calculations. The details of this “bootstrap” procedure have been described previously,²⁴ and it is functionally equivalent to the FABM method of Teo et al.²⁶

Results

The nickel K absorption edge regions for a number of Ni(II) compounds are compared in Figure 1. Relatively little analysis of Ni absorption edges has appeared, but a qualitative interpretation similar to that of other transition-metal edges is an appropriate starting point.²⁷ For nickel complexes the first edge

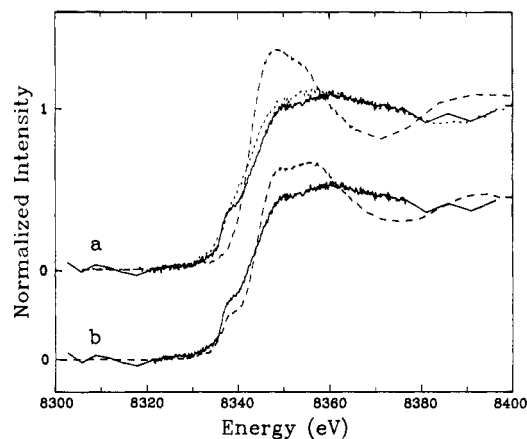


Figure 2. Nickel absorption edge region: (a) rubredoxin-oxidized *C. thermoacetium* CO dehydrogenase (—) compared to the nickel edge of *S*-methyl reductase from *M. thermoautotrophicum*, strain ΔH (---), and *D. gigas* hydrogenase (---); (b) rubredoxin-oxidized COdH (—) vs. F_{430} (---).

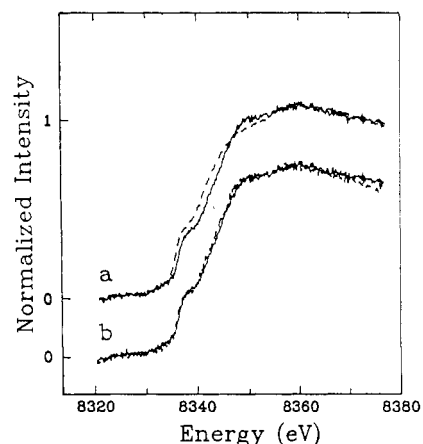


Figure 3. Nickel absorption edge region for COdH under various conditions: (a) rubredoxin-oxidized (—) vs. hydrogenase/ H_2 -reduced COdH (---); (b) rubredoxin-oxidized (—) vs. oxidized COdH + CO (---).

feature is the forbidden $1s \rightarrow 3d$ transition, usually a very weak peak at ~ 8333 eV. The next feature at ~ 8338 eV is variously described as a $1s \rightarrow 4s$ transition,²⁷ a $1s \rightarrow 4p$ plus shakedown transition,²⁸ or a $1s \rightarrow 4p_z$ transition.^{17,29} The features between 8348 and 8370 eV can be qualitatively described as $1s \rightarrow 4p$ and $1s \rightarrow 5p$ transitions,²⁷ but more sophisticated XANES calculations have shown that this part of the edge must be described in terms of multiple scattering resonances.³⁰

The data presented in Figure 1 illustrate the sensitivity of nickel edges to the type of ligand and the metal site symmetry. Figure 1a shows that the tentatively assigned “ $1s \rightarrow 4p_z$ ” transition is strong and well resolved in square-planar complexes. Comparison of spectra for $\text{Ni}^{\text{II}}(\text{ibc})$ (square-planar NiN_4) and $[\text{Ni}^{\text{II}}(\text{mnt})_2]^{2-}$ (square-planar NiS_4) shows that this transition occurs at slightly lower energy and with somewhat increased intensity in the case of Ni-S coordination. It is also clear that the maximum height of the normalized edge is greater in the compound with nitrogen as opposed to sulfur donor ligands. This relationship is also observed for the octahedral models of Figure 1b, where the edge maximum of nitrogen-based $[\text{Ni}^{\text{II}}(\text{en})_3]^{2+}$ is significantly higher than for the sulfur-coordinated $[\text{Ni}^{\text{II}}(\text{[9]aneS}_3)_2]^{2+}$ model. In the model with tetrahedral geometry, $[\text{Ni}^{\text{II}}(\text{SC}_6\text{H}_5)_4]^{2-}$, the strong

(17) Eidsness, M. K.; Sullivan, R. J.; Schwartz, J. R.; Hartzell, P. L.; Wolfe, R. S.; Flank, A.-M.; Cramer, S. P.; Scott, R. A. *J. Am. Chem. Soc.* **1986**, *108*, 3120–3121.

(18) Scott, R. A.; Wallin, S. A.; Czechowski, M.; DerVartanian, D. V.; LeGall, J.; Peck, H. D., Jr.; Moura, I. *J. Am. Chem. Soc.* **1984**, *106*, 6864–6865.

(19) Cramer, S. P.; Scott, R. A. *Rev. Sci. Instrum.* **1981**, *52*, 395–399.

(20) Cramer, S. P.; Wahl, R.; Rajagopalan, K. V. *J. Am. Chem. Soc.* **1981**, *103*, 7721–7727.

(21) Cramer, S. P. In *EXAFS for Inorganic Systems*, Garner, C. D., Hsain, S. S., Eds.; Daresbury Laboratory: Daresbury, England, 1981; pp 47–50.

(22) Cramer, S. P.; Hodgson, K. O.; Stiefel, E. I.; Newton, W. E. *J. Am. Chem. Soc.* **1978**, *100*, 2748–2761.

(23) Cramer, S. P.; Solomonson, L. P.; Adams, M. W. W.; Mortenson, L. E. *J. Am. Chem. Soc.* **1984**, *106*, 1467–1471.

(24) Cramer, S. P.; Hille, R. *J. Am. Chem. Soc.* **1985**, *107*, 8164–8169.

(25) Teo, B. K.; Lee, P. A. *J. Am. Chem. Soc.* **1979**, *101*, 2815–2832.

(26) Teo, B. K.; Antonio, M. R.; Averill, B. A. *J. Am. Chem. Soc.* **1983**, *105*, 3751–3762.

(27) Shulman, R. G.; Yafet, Y.; Eisenberger, P.; Blumberg, W. E. *Proc. Natl. Acad. Sci. U.S.A.* **1976**, *73*, 1384–1388.

(28) Kosugi, N.; Yokoyama, T.; Asakura, K.; Kuroda, H. *Chem. Phys.* **1984**, *91*, 249–256. Yokoyama, T.; Kosugi, N.; Kuroda, H. *Chem. Phys.* **1986**, *103*, 101–109.

(29) Smith, T. A.; Penner-Hahn, J. E.; Berding, M. A.; Doniach, S.; Hodgson, K. O. *J. Am. Chem. Soc.* **1985**, *107*, 5945–5955.

(30) Kutzler, F. W.; Natoli, C. R.; Misemer, D. K.; Doniach, S.; Hodgson, K. O. *J. Chem. Phys.* **1980**, *73*, 3274–3288.

1s → 3d transition is clearly observed at 8331 eV, as illustrated in Figure 1c.

The COdH Ni edge spectrum is different from the edge spectra observed for other nickel-containing enzymes. These differences are illustrated in Figure 2a for COdH, the *M. thermoautotrophicum* S-methyl reductase, and the *D. gigas* hydrogenase. The COdH edge has a transition near 8338 eV (tentatively assigned as the 1s → 4p_z transition), which is absent in the spectra of the other enzymes. However, the remainder of the COdH edge is similar to the hydrogenase edge in shape and peak height. In Figure 2b, the Ni edge region for COdH is compared with that of the Ni-containing factor F₄₃₀ isolated from S-methyl reductase.¹⁷ Although both of these spectra exhibit resolved shoulders, at higher energies the increased intensity of the F₄₃₀ spectrum maximum is consistent with nitrogen ligation, while the reduced intensity of the COdH edge suggests the presence of sulfur ligation.

Figure 3a illustrates the changes in the nickel edge region observed after treatment of the rubredoxin-oxidized enzyme with a reducing system consisting of hydrogenase/H₂. This treatment causes the edge to shift to lower energy, consistent with the nickel becoming more reduced. However, there is no Ni EPR signal to monitor for these samples, and the X-ray edge data alone cannot tell what fraction of the nickel is affected. Nevertheless, the edge shift suggests that the nickel is redox active and can be reduced from the rubredoxin-oxidized state to a lower oxidation state. Addition of CO to rubredoxin-oxidized COdH results in insignificant changes in the edge features (Figure 3b). When CO was bound, this sample yielded an EPR signal that integrated to 48% of the nickel in the sample. Since virtually no edge shift accompanied the appearance of this CO-induced EPR signal, the fraction of nickel site(s) responsible for the EPR signal has not undergone major changes in coordination environment nor valence state upon CO binding.

Our preliminary Ni EXAFS data on rubredoxin-oxidized COdH extend over the limited range of $k = 3.5\text{--}10.5 \text{ \AA}^{-1}$. Curve fitting the data from $k = 4\text{--}10 \text{ \AA}^{-1}$ suggests that the major features in the EXAFS can be approximated by a single Ni-S component or a combination of Ni-S and Ni-(N,O) components. The best fit is achieved with approximately two Ni-S bonds at 2.21 Å and approximately two Ni-(N,O) bonds at 1.97 Å. The present range of EXAFS data does not lead to a unique structure.

Discussion

To understand the structure and function of the nickel site in COdH, it is important to know the types of ligands and the geometry of their arrangement about the nickel center. The current results can be used to eliminate certain candidate structures, but they do not identify unique solutions. The most important XANES result is the moderate intensity of the transition at ~8338 eV. Given the presence of S-containing nickel ligands (as determined by EXAFS), the intensity is probably too weak to result from a strictly square-planar environment and is too strong for an octahedral or a tetrahedral site. A tetrahedral geometry is unlikely also owing to the weakness of the 1s → 3d transition. The best candidates are distorted-square-planar or square-pyramidal geometries, based on analogy with Cu edges that exhibit weaker, less well-defined, shoulders for these intermediate geometries.^{29,30}

The short range of the useful EXAFS data limits the information that can be obtained about the COdH Ni ligands. Preliminary curve-fitting results suggest that both Ni-(N,O) and Ni-S interactions may be present at the Ni site; a more extended range of data is needed to confirm this possibility. The overall height of the oxidized COdH edge suggests that at least some of the ligands are bound to nickel through sulfur atoms, consistent with the curve-fitting results.

The nickel environment in CO dehydrogenase can now be compared with the three other known enzymatic nickel species:

jackbean urease, (Ni,Fe)-hydrogenases, and S-methyl coenzyme-M reductase. Hasnain and Piggott have reported XAS data for jackbean urease that resemble data for a model compound with nitrogen and oxygen ligands in an octahedral environment.³¹ However, the data were presented in a manner such that the correspondence could only be confirmed to about 250 eV beyond the edge ($k = 8 \text{ \AA}^{-1}$). Lindahl et al. have reported the EXAFS of the F₄₂₀-reducing hydrogenase from *M. thermoautotrophicum*.³² Their useful data, which extended to $k = 8.8 \text{ \AA}^{-1}$, yielded an average Ni-S distance of $2.25 \pm 0.04 \text{ \AA}$ with a large rms deviation (Debye-Waller σ) of 0.09 Å. They reported an amplitude corresponding to approximately three sulfurs, and they suggested that additional ligands are probably present. Scott and coworkers have reported the edge and EXAFS spectra for the nickel in the hydrogenase from *D. gigas*.¹⁸ They derived an average Ni-S distance of $2.20 \pm 0.02 \text{ \AA}$ with an amplitude corresponding to about four sulfurs and again a large σ .³³ Finally, the data for S-methyl reductase¹⁷ indicate that the Ni coordination sphere in the intact protein consists of a single Ni-N distance of 2.09 Å. Some forms of isolated F₄₃₀, however, show a distorted first coordination sphere with nitrogen ligands at 1.9 and 2.1 Å.^{17,34}

In general, XAS data of the COdH nickel site resemble data for hydrogenase more than they resemble the data for the F₄₃₀-based structures. Our preliminary work suggests that the Ni coordination sphere geometry may be distorted square planar or square pyramidal. The EXAFS data do not present a definitive solution, but the best fits come from simulations with both Ni-(N,O) and Ni-S interactions. It is clear, however, that compared to the nickel in other nickel metalloenzymes, the nickel in COdH exists in a structurally unique environment.

Acknowledgment. The following people are gratefully acknowledged for supplying the indicated Ni compounds for this study: [(C₆H₅)₄P]₂[Ni(SC₆H₅)₄], Dimitri Coucouvanis; Ni(IBC), Jack Fajer; [Ni([9]aneS₃)₂](ClO₄)₂, Karl Wieghardt. The XAS data were collected at the Stanford Synchrotron Radiation Laboratory (SSRL), which is supported by the Office of Basic Energy Sciences, Department of Energy, and the Biotechnology Resource Program, Division of Research Resources, National Institutes of Health. XAS work at the University of Illinois under R.A.S. is supported by the NSF (Grant DMB 85-02707). R.A.S. is a NSF Presidential Young Investigator (1985-1990) and an Alfred P. Sloan Research Fellow (1986-1988). Research at the University of Georgia under L.G.L. is supported by the U.S. Department of Energy (Grant DE-AS 09-79ER10499) and the National Institutes of Health (Grant MBC 5 R01 DK27323).

Registry No. COdH, 64972-88-9; Ni^{II}(Et₂dtc)₂, 14267-17-5; Ni^{II}(IBC), 96866-34-1; [(*n*-C₄H₉)₄N]₂[Ni^{II}(mnt)₂], 18958-57-1; [Ni^{II}(en)₃]Cl₂, 13408-70-3; [Ni^{II}([9]aneS₃)₂](ClO₄)₂, 97465-53-7; [(C₆H₅)₄P]₂[Ni^{II}(S-C₆H₅)₄], 57927-74-9; Ni, 7440-02-0.

Supplementary Material Available: Tables of raw Ni XAS data for the three COdH samples (rubredoxin-oxidized, hydrogenase/H₂-reduced, oxidized + CO) and for Ni compounds [Ni(IBC)], [(*n*-C₄H₉)₄N]₂[Ni(mnt)₂], [Ni(en)₃]Cl₂, [Ni([9]aneS₃)₂](ClO₄)₂, and [(C₆H₅)₄P]₂[Ni(S-C₆H₅)₄] (25 pages). Ordering information is given on any current masthead page.

- (31) Hasnain, S. S.; Piggott, B. *Biochem. Biophys. Res. Commun.* **1983**, *112*, 279-283.
- (32) Lindahl, P. A.; Kojima, N.; Hausinger, R. P.; Fox, J. A.; Teo, B. K.; Walsh, C. T.; Orme-Johnson, W. H. *J. Am. Chem. Soc.* **1984**, *106*, 3062-3064.
- (33) Scott et al.¹⁸ reported the Ni-S Debye-Waller factor as $\Delta\sigma^2 = 0.0052 \text{ \AA}^2$ where the difference is with respect to the [Ni(mnt)₂]⁻ model compound. If the absolute σ^2 for the model is assumed to be 0.0026 Å² (calculated from the Ni EXAFS fit with a scaled theoretical amplitude envelope), then the absolute σ^2 for the protein data would be 0.0078 Å², close to the value reported by the other group.³²
- (34) Diakun, G. P.; Piggott, B.; Tinton, H. J.; Ankel-Fuchs, D.; Thauer, R. K. *Biochem. J.* **1985**, *232*, 281-284.